Basic Co-rich decagonal Al-Co-Ni: Average structure

Angelica Strutz,[1,*] Akiji Yamamoto,[2,†] and Walter Steurer[1,‡]
[1]*Laboratory of Crystallography, Department of Materials, ETH Zurich, 8093 Zurich, Switzerland*
[2]*National Institute for Materials Science, Namiki 1, Tsukuba, Ibaraki 305-0044, Japan*
(Received 4 August 2009; published 10 November 2009)

The two-layer average structure of the high-temperature phase basic Co-rich decagonal $Al_{72.5}Co_{18.5}Ni_9$ was determined based on single-crystal x-ray diffraction data. The five-dimensional (5D) structure model was refined in the noncentrosymmetric 5D space group $P\bar{1}0m2$ (112 parameters, $wR=0.123$ and $R=0.156$ for 957 reflections). The close relationship of the model structure with that of W-Al-Co-Ni, a $\langle 3/2,2/1\rangle$ approximant, is shown.

DOI: 10.1103/PhysRevB.80.184102 PACS number(s): 61.05.cp, 61.44.Br, 61.66.Dk

I. INTRODUCTION

Understanding formation, stability, and physical properties of quasicrystals requires the knowledge of their structures. Furthermore, some of the structure/property relationships of quasicrystals, which are mostly intermetallic phases, are not only of interest in their own right, but also, increasingly, for the design of photonic and phononic crystals.[1] However, of the more than 70 stable quasicrystals discovered so far, the structures of only a handful of them have been determined yet due to the intricate complexity of quasicrystal structure analysis.[2,3]

Decagonal quasicrystals, i.e., quasicrystals with decagonal diffraction symmetry, can geometrically be described either as periodic stacking of quasiperiodic atomic layers or as packing of decagonal clusters. From the viewpoint of chemical bonding, however, decagonal quasicrystals are by no means layer structures and the term cluster has to be understood just as a synonym for structural building unit.[4,5]

The system Al-Co-Ni is an excellent model system for the study of the influence of chemical composition on the formation of different quasicrystal modifications and approximants.[6] As a function of the Co/Ni ratio, different superstructures form either in the quasiperiodic directions or along the periodic tenfold axis.[7] Though Co and Ni are next to each other in the periodic table differing by only one *d* electron, the x-ray diffraction patterns of those modifications show significant variations.[8] This indicates significant structural changes accompanying Co/Ni ordering with the variation in their ratio. Indeed, quantum-mechanical model calculations showed local rearrangements of coordination polyhedra depending on the kind of TM atoms present.[9]

Basic Co-rich decagonal-Al-Co-Ni (d-Al-Co-Ni), stable between approximately 840 and 1060 °C, possesses a twofold superstructure along the tenfold axis, doubling the two-layer periodicity present in the basic Ni-rich modification. This kind of superstructure is also present in all other d-Al-Co-Ni modifications as well as in d-Al-Co-Cu. However, only in the basic Co-rich modification it has the long-range correlation needed for single-crystal x-ray structure analysis. In other words, only in basic Co-rich d-Al-Co-Ni the superstructure reflections are sharp Bragg reflections, in all other cases they are diffuse, indicating a correlation length of a few cluster diameters only.[8]

While all modifications have already been investigated by electron microscopy,[10] quantitative single-crystal x-ray diffraction structure analyses have only been performed so far for the basic Ni-rich phase[11–13] as well as for the average structure of the superstructure of type II.[14] In a more qualitative manner, basic Co-rich d-Al-Co-Ni has as well been modeled based on x-ray diffraction data.[15,16] Electron microscopy can only provide projected structural information, therefore it can be highly valuable for identifying clusters and underlying tilings but it cannot give a full, quantitative picture of the three-dimensional (3D) structure. This is the domain of single-crystal x-ray diffraction methods, and this is the goal of our study.

In the following we present the refined five-dimensional (5D) model of the average structure of basic Co-rich d-$Al_{72.5}Co_{18.5}Ni_9$. This represents the first part of the tedious determination of its full structure based on single-crystal x-ray diffraction data. A 5D model[17] of d-Al-Fe-Ni with four-layer periodicity has been used as basis for our 5D starting model. The good fit between observed and calculated x-ray diffraction intensities as well as the convincing agreement with the projected structure of the closely related W phase, a rational approximant, prove the validity of the proposed structure solution. Since quasicrystals and their structurally closely related approximants consist of the same atomic clusters, the four-layer structure of the W phase gives valuable information on the twofold superstructure of basic Co-rich d-$Al_{72.5}Co_{18.5}Ni_9$, which will be presented in a follow-up paper.

II. EXPERIMENT

For sample preparation, compacts with composition $Al_{72.5}Co_{18.5}Ni_9$, 1g each, were pressed from pulverized Al (Heraeus 99.95 wt %), Co (Alfa Aesar 99.8 wt %) and Ni (Heraeus 99.99 wt %) in argon atmosphere (Mbraun glove box 150 B-G, PanGas Ar 99.998). Prealloys were prepared by melting the compacts in an arc furnace (DEGUSSA VOLi O) with nonconsumable tungsten electrode under Ti-gettered argon. The as-cast samples were analyzed by differential temperature analysis (DTA) (Perkin Elmer DTA 7) using Al_2O_3 crucibles under high-purity argon (cooling rates of 10 °C/min). Quasicrystal growth and annealing was performed in a high-vacuum resistance furnace (PVA MOV 64).

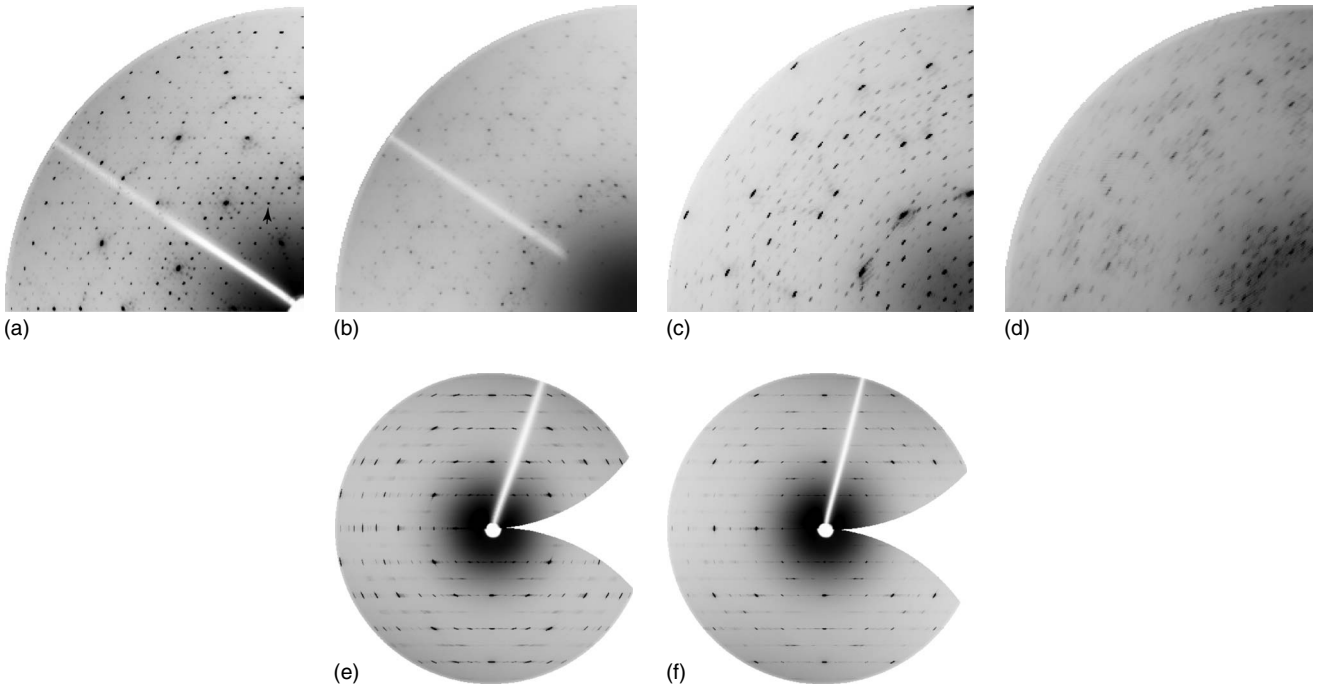

FIG. 1. Reciprocal space sections of decagonal $Al_{72.5}Co_{18.5}Ni_9$ reconstructed from 180 image-plate-scanner frames each: $h_1h_2h_3h_4h_5$ with (a) $h_5=0$, (b) $h_5=1$, (c) $h_5=2$, (d) $h_5=3$ [h_5 referring to the four-layer 8.16(4) Å period], (e) $h_1h_2\bar{h}_2\bar{h}_1h_5$, and (f) $h_1h_2h_2h_1h_5$. The sections in (b) and (d) contain superstructure reflections only. The reflection 10000 [Yamamoto setting (Ref. 18)] is marked by an arrow in (a).

Therein, an as-cast sample was heated in an Al_2O_3 crucible to 1350 °C (i.e., above melting temperature), held at this temperature for 20 min, then cooled to 1000 °C with a cooling rate of 0.24 °C/min and subsequently annealed for 48 h at 1000 °C. Eventually, the sample was quenched by jetting cold argon into the sample chamber.

Single crystal x-ray data were collected at SNBL/ESRF Grenoble, using a marresearch 345 imaging-plate scanner (180 frames with an oscillation angle of $\phi=1°$ each, wavelength $\lambda=0.72326$ Å). Two data sets were collected, *data set* 1 with an exposure time of 4 s/frame to prevent saturation of strong reflections, data set 2 with 100 s/frame in order to detect a sufficient amount of the rather weak superstructure reflections. The reciprocal space layers $h_1h_2h_3h_4h_5$ with $h_5=0$, 1, 2, and 3, and the reciprocal space sections $h_1h_2h_2h_1h_5$ and $h_1h_2\bar{h}_2\bar{h}_1h_5$, perpendicular to them as well as to each other and containing the tenfold axis, are shown in Fig. 1.

Since the strongest reflections of these two synchrotron data sets are still oversaturated, additionally an in-house data set (data set 3) was collected employing a four-cycle diffractometer equipped with a charge-coupled device detector (Oxford Diffraction Xcalibur, $7.5° \leq 2\theta \leq 55.5°$, 360 frames with $\phi=1°$ each, exposure time 10 s/frame, 50 kV, 40 mA, graphite monochromatized Mo$K\alpha$ radiation).

Data reduction was performed using the software package CRYSALIS (Oxford Diffraction). According to the observed Laue symmetry $10/mmm$, data set 1 with 39 315 reflections was merged into 1405 unique reflections with $R_{int}=0.174$, data set 2 with 41 810 reflections was merged into 1434 unique reflections with $R_{int}=0.163$ and data set 3 with 899 034 reflections was merged into 1764 unique reflections with $R_{int}=0.098$. The index of the strongest reflection in the zero layer is 13420 in the Yamamoto setting[18] (02210 in the Steurer setting[6]) that is used throughout the paper [see Fig. 1(a)]. The three data sets were scaled to each other using QCDIFF, a refinement program for quasicrystal structures included in the program package QUASI07_08.[19]

III. 5D MODEL BUILDING

The reconstructed reciprocal space layers (Fig. 1) show quite different intensity distributions in even and odd layers perpendicular to the tenfold axis. The even layers consist of main reflections only that can be indexed using the basis of the basic Ni-rich phase. These reflections contain the information on the two-layer average structure. The superstructure reflections, which are only present in the odd layers and result from some modifications in the average structure, cannot be indexed on the same basis. The reciprocal basis of the superstructure of type I (Ref. 20) can be used as a common basis for both main and satellite reflections. It can be obtained from that of the basic structure by rotoscaling, i.e., a rotation by $\pi/10$ and scaling by a factor of $1/[2\cos(\pi/10)]=0.5257$. In the present analysis of the average structure, however, only the main reflections are included in the refinements.

With the parameters $a_o=2.745(2)$ Å [defined by the 10000 reflection marked in Fig. 1(a)] and $c_o=4.072(1)$ Å (along the tenfold axis), we obtain a proper 5D basis (Yamamoto setting[21]) for the main reflections

$$\mathbf{d}_j^* = \frac{a_o^*}{\sqrt{5}}[c_j\mathbf{a}_1 + s_j\mathbf{a}_2 + c_{2j}\mathbf{a}_3 + s_{2j}\mathbf{a}_4]$$

$$\text{for } j=1,\ldots,4 \text{ and } \mathbf{d}_5^* = c_o^*\mathbf{a}_5 = \mathbf{c}_o^* \qquad (1)$$

and reciprocal to it

$$\mathbf{d}_j = \frac{2a_o}{\sqrt{5}}[(c_j - 1)\mathbf{a}_1 + s_j\mathbf{a}_2 + (c_{2j} - 1)\mathbf{a}_3 + s_{2j}\mathbf{a}_4]$$

$$\text{for } j = 1, \ldots, 4 \text{ and } \mathbf{d}_5 = c\mathbf{a}_5 = \mathbf{c}_o, \tag{2}$$

where $a_o^* = 1/a_o$, $c_o^* = 1/c_o$, $c_j = \cos(2\pi j/5)$, $s_j = \sin(2\pi j/5)$, $c_2 j = \cos(4\pi j/5)$, and $s_2 j = \sin(4\pi j/5)$. The vectors $\mathbf{a}_1$, $\mathbf{a}_2$, and $\mathbf{a}_5$ are external space unit vectors and $\mathbf{a}_3$ and $\mathbf{a}_4$ internal space unit vectors.

A symmetry analysis of the full reflection data set reveals the Laue symmetry $10/mmm$. Neglecting some weaker reflections, one finds an extinction rule for the superstructure, $h_1 h_2 \bar{h}_2 \bar{h}_1 h_5$ with $h_5 = 2n+1$ indicating a pseudo-5D c-glide plane for the four-layer superstructure. Considering the pseudosymmetry as true symmetry, possible space groups would either be centrosymmetric $P10_5/mmc$ or noncentrosymmetric $P\bar{1}02c$, otherwise $P10/mmm$ or $P\bar{1}02m$, respectively.

If we take the pseudosymmetry into account, then the projection of the four-layer superstructure onto the two-layer average structure changes the symmetry from $P10_5/mmc$ to $P10/mmm$, and from $P\bar{1}02c$ to $P\bar{1}02m$. If we consider the true symmetry of the four-layer structure for the average structure we end up with $P10/mmm$ or $P\bar{1}02m$, respectively, as well. For the average structure described by the basis of the basic Ni-rich phase, the mirror plane is rotated by $\pi/10$ relatively to the superstructure basis. Hence the higher dimensional space group is $P\bar{1}0m2$.

The structure of a decagonal quasicrystal can be described as an external space cut of a 5D periodic hypercrystal structure with basis $\mathbf{d}_j$, $j=1,\ldots,5$. The structural information is coded in two-dimensional occupation domains (OD), which are parallel to internal space. A starting model for the structure refinements has been obtained by the low-density elimination method.[22] The principle behind this powerful iterative direct-space approach is that all (electron) density values below a given threshold value δ are set to zero. The OD identified in this way are centered at the special positions (1,1,1,1,5/4)/5, (2,2,2,2,5/4)/5, (4,4,4,4,15/4)/5, (3,3,3,3,15/4)/5, (0,0,0,0,1/4), and (0,0,0,0,3/4). The two OD at (0,0,0,0,1/4) and (0,0,0,0,3/4) have an external space distance of only 2.04 Å. Consequently, they will generate partially occupied (split) positions with partial occupancies summing up to at most one.

For the structure refinements the obtained density distribution has to be properly parameterized by polygonal subdomains.[17,18] Due to the similarity between the observed diffraction patterns of basic Co-rich d-Al-Co-Ni and the simulated diffraction pattern of d-Al-Ni-Fe, this could be done based on Yamamoto's model for d-Al-Fe-Ni.[17] For that purpose, five internal space basis vectors are defined

$$\mathbf{v}_j = \frac{2a_o}{\sqrt{5}}[c_{2j}\mathbf{a}_3 + s_{2j}\mathbf{a}_4], \quad j = 1, \ldots, 5 \tag{3}$$

with $2a_o/\sqrt{5} = 2.43$ Å. Each vector is parallel to one of the center-to-vertex vectors of a reference pentagon. The vector $\mathbf{v}_5$ is redundant, since it can be expressed as a linear combination of the other four vectors, $\mathbf{v}_5 = -(\mathbf{v}_1 + \mathbf{v}_2 + \mathbf{v}_3 + \mathbf{v}_4)$. The vectors $\mathbf{v}_j$ $(j=1,\ldots,4)$ are equal to the internal space components of the decagonal lattice vectors $\mathbf{d}_j - \mathbf{v}_5$. Note that $\mathbf{d}_5$ is parallel to the tenfold axis in external space. By using $\mathbf{v}_j$ as unit vectors, the ith corner vector of an OD is written as $\mathbf{e}_i = (x_1, x_2, x_3, x_4, x_5)$.

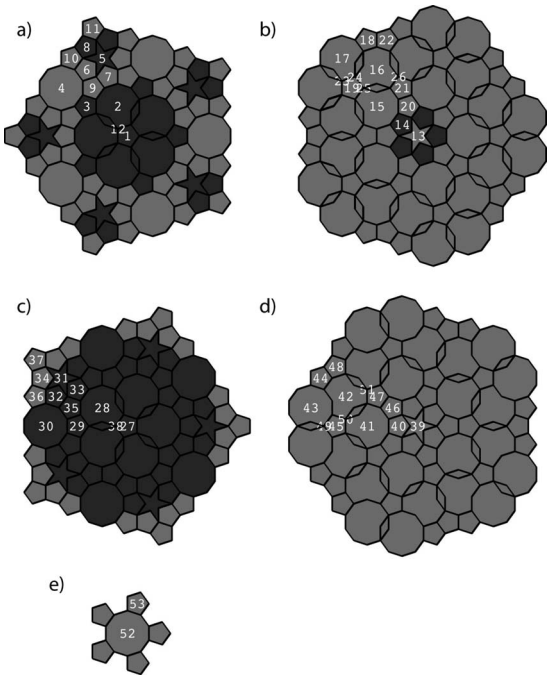

FIG. 2. Independent OD of the refined model structure of Co-rich d-Al-Co-Ni, located at (a) (1,1,1,1,5/4)/5, (b) (2,2,2,2,5/4)/5, (c) (4,4,4,4,15/4)/5, (d) (3,3,3,3,15/4)/5, and (e) (0,0,0,0,3/4). Dark gray indicates TM atoms (Co or Ni) and light gray Al atoms.

The number of atoms per unit cell, a hard constraint for modeling in standard structure analysis, is not available for quasiperiodic structures. Its role is taken over by the point density, i.e., the inverse of the average atomic volume, which can be derived from the mass density of the quasicrystal. This quantity is convenient for checking the quality of a model also during the refinement steps since the point density can be expressed as the ratio between the total area of the occupation domains times their individual occupancies and the 5D unit-cell volume.

Lacking convergent-beam electron-diffraction information, it was not possible to decide whether or not the average structure has an inversion center. Therefore, five independent OD were used. Since the final distribution of the Al and TM atoms strongly deviates from the centrosymmetric case, we conclude that the 5D space group is $P\bar{1}0m2$ indeed. The point density of the model is $\rho' \approx 0.073$ Å^{-3}.

IV. STRUCTURE REFINEMENT

Since it is hardly possible to distinguish between Co and Ni based on x-ray diffraction data, the structure has been refined as a pseudobinary phase containing just Al and TM atoms. For the latter atomic scattering factors of Co were used. It may be possible to comment on the Co/Ni ordering once the full structure of basic Co-rich decagonal Al-Co-Ni will have been solved by drawing conclusions from the ordering in W-Al-Co-Ni. There, the influence of Co and Ni

TABLE I. Basic polygons defining the subdomains partitioning the large OD (Fig. 2). The superscript i refers to the internal space component. $\tau=(1+\sqrt{5})/2$.

Polygon	Corner vectors defining the polygonal	Subdomains	
Decagon	$\mathbf{e}_1=(0,\tau^{-4},-\tau^{-4},0,0)^i$	$\mathbf{e}_2=(-\tau^{-4},\tau^{-4},0,0,0)^i$	$\mathbf{e}_3=(-\tau^{-4},0,0,0,\tau^{-4})^i$
Pentagon	$\mathbf{e}_1=\tau^{-5}(0.4,0.4,-0.6,-0.4,-0.6)^i$	$\mathbf{e}_2=\tau^{-5}(-0.6,0.4,-0.6,0.4,0.4)^i$	$\mathbf{e}_3=\tau^{-5}(-0.6,0.4,0.4,-0.6,0.4)^i$
	$\mathbf{e}_4=\tau^{-5}(0.4,-0.6,0.4,-0.6,0.4)^i$	$\mathbf{e}_5=\tau^{-5}(0.4,-0.6,0.4,0.4,-0.6)^i$	
Star	$\mathbf{e}_1=\tau^{-5}(-0.2,0.8,-1.2,0.8,-0.2)^i$	$\mathbf{e}_2=\tau^{-5}(0.43,0.43,-0.43,0.0,-0.43)^i$	$\mathbf{e}_3=\tau^{-5}(0.8,-0.2,-0.2,0.8,-1.2)^i$
Rhombus	$\mathbf{e}_1=(\tau^{-5},-\tau^{-5},0,0,0)^i$	$\mathbf{e}_2=(2\tau^{-5},-\tau^{-5},0.0,0.0,-\tau^{-5})^i$	$\mathbf{e}_3=(\tau^{-5},0.0,0.0,0.0,-\tau^{-5})^i$

atoms on their local atomic coordinations has been studied by quantum-mechanical calculations[9] as well as by neutron diffraction.[23]

The final model contains five OD subdivided into 53 independent subdomains (Fig. 2) based on the basic polygons listed in Table I. During the refinement process various modifications were required for the subdivision of the OD as well as for the chemical occupancies of the subdomains. The OD in (0,0,0,0,1/4) had to be removed because its occupancy refined to zero. The final Al/TM distribution is illustrated in Fig. 2 and Table III.

For each subdomain in the current model, the external space displacements u_1 and u_2 from their ideal positions and Al/TM ratio (mixing parameter s_1) were refined. Overall external space atomic-displacement parameters (ADP, "Debye-Waller factor"), $B_{\|}$ within the quasiperiodic plane and $B_{\perp}$ perpendicular to it, were refined for each OD ($B=8\pi^2\langle u^2\rangle$, with u as the displacement amplitude). The refinement of individual ADP from each subdomain was not possible due to the limited number of reflections.

The center of a subdomain is displaced by the internal space vector $\mathbf{x}^i$ relative to the center $\mathbf{x}_0$ of the OD hence the actual position of each subdomain is $\mathbf{x}_0+\mathbf{x}^i$. Taking into consideration symmetry restrictions, we identified for each subdomain possible external space shift vectors, $\mathbf{x}_1^e$ and $\mathbf{x}_2^e$, defined on the basis

$$\mathbf{u}_j=\frac{2a_o}{\sqrt{5}}[c_j\mathbf{a}_1+s_j\mathbf{a}_2],\quad (j=1,\ldots,5),\quad \mathbf{u}_6=\mathbf{a}_3. \qquad (4)$$

The number of shift vectors for the individual subdomains is restricted by site symmetry to maximum two (Table II). In this case the position of a displaced subdomain is given by $\mathbf{x}=\mathbf{x}_0+\mathbf{x}^i+u_1[\mathbf{x}_1^e/|\mathbf{x}_1^e|]+u_2[\mathbf{x}_2^e/|\mathbf{x}_2^e|]$. The displacements resulting from the refinements are listed in Table III.

The refined parameters for each individual subdomain are summarized in Table III. For each subdomain are given its relative position $\mathbf{x}^i$, external space displacements u_1 and u_2, and partial occupancy factor p, where all subdomains are fully occupied. $B_{\|}$ and $B_{\perp}$ components of the ADP are given for each OD. The estimated standard deviation (esd) for each refined parameter is less or equal 0.01.

Scaling factors and two parameters for the secondary extinction factor were refined as common parameters for all subdomains and individually for each diffraction data set. In addition, a phason displacement parameter ("phason Debye-Waller factor") was refined to $b_i=0.112(2)$ Å^2 for the synchrotron data with weak reflections.

Three penalty functions were included, PF_1 for occupation probabilities, PF_2 for the displacement parameter, and PF_3 for the chemical composition. Their weights were chosen to be 0.5, 0.3, and 0.3, respectively. In the framework of the present structure solution the final model was refined with a chemical composition of $Al_{72.3}TM_{27.7}$ compared to the actual one of $Al_{72.5}(Co,Ni)_{27.5}$. The final R values are $wR=0.123$ and $R=0.156$ for 957 unique reflections based on three data sets. The high quality of the fit is reflected in the F_{obs}/F_{calc} distribution shown in Fig. 3.

Not all the reflections from the three data sets were included in the refinement process. Our threshold parameters are based on $\sigma|F_o|$, which is $\sigma|F_o|=\sqrt{\sigma(F_o^2)}/2$ for strong reflections and $\sigma|F_o|=\sigma(F_o^2)/2|F_o|$ for weak reflections.[24] The resulting R factors of the partial subsets are: $wR=0.040$ and $R=0.094$ for data set 1 with strong reflections

TABLE II. Symmetry allowed shift vectors of the subdomains shown in Fig. 2. The superscript e indicates that the shifts only have external space components.

Subdomain	Shift vector $\mathbf{x}_1^e$	Shift vector $\mathbf{x}_2^e$
1, 13, 27, 39, 52		
2, 5, 7, 11, 20, 21, 22, 26	$(0,-1,0,0,0,0)^e$	
3, 4, 12, 14, 15, 17, 19, 23, 28, 31, 33, 37, 46, 47, 48, 51	$(1,0,0,0,0,0)^e$	
29, 30, 38, 40, 41, 45, 49	$(0,0,0,0,-1,0)^e$	
53	$(0,0,1,0,0,0)^e$	
6, 8, 9, 10, 16, 17, 18, 24, 25	$(1,0,0,0,0,0)^e$	$(0,-1,0,0,0,0)^e$
32, 34, 35, 36, 42, 43, 44, 50	$(1,0,0,0,0,0)^e$	$(0,0,0,0,-1,0)^e$

TABLE III. Refined parameters: external space shifts of the subdomains u_1, u_2, ADP components $B_\parallel$ and $B_\perp$, and partial occupancy factors p for TM and Al; esds of refined parameters are all less or equal 0.01; and fixed parameters are marked by *.

Subdomain: $\mathbf{x}^i$	u_1 (Å)	u_2 (Å)	$B_\parallel$ (Å^2)	$B_\perp$ (Å^2)	p(TM)	p(Al)
OD1: $\mathbf{x}_0=(0.2,0.2,0.2,0.2,0.25)$			0.73	1.27		
1: $(0,0,0,0,0,0)^i$					0.93	0.07
2: $\tau^{-1}(0.4,0.4,0.4,-0.6,-0.6,0)^i$	0.07				1.00	0.00
3: $\tau^{-1}(0.8,-0.2,-0.2,-0.2,-0.2,0)^i$	−0.01				0.84	0.16
4: $\tau^{-1}(0.4,-0.6,0.4,0.4,-0.6,0)^i$	0.13				0.24	0.76
5: $\tau^{-1}(0.6,-0.4,0.6,-0.4,-0.4,0)^i$	0.16				1.00	0.00
6: $\tau^{-1}(-0.2,-1.2,0.8,0.8,-0.2,0)^i$	0.01	0.21			0.32	0.68
7: $\tau^{-1}(0.8,0.8,0.8,-1.2,-1.2,0)^i$	0.05				0.29	0.71
8: $\tau^{-1}(1.8,-0.2,-0.2,-1.2,-0.2,0)^i$	−0.10	−0.22			0.75	0.25
9: $\tau^{-1}(0,0,1,0,-1,0)^i$	0.08	−0.01			0.00	1.00
10: $\tau^{-1}(1,-1,0,0,0,0)^i$	0.09	0.16			0.00	1.00
11: $\tau^{-1}(1,0,1,-1,-1,0)^i$	0.24				0.00	1.00
12: $\tau^{-5}(0.4,-0.6,0.4,0.4,-0.6,0)^i$	0.02				1.00	0.00
OD2: $\mathbf{x}_0=(0.4,0.4,0.4,0.4,0.25)$			0.88	6.54		
13: $(0,0,0,0,0,0)^i$					0.49	0.51
14: $\tau^{-1}(1.2,0.2,-0.8,-0.8,0.2,0)^i$	0.07				0.41	0.59
15: $\tau^{-1}(0.8,-0.2,-0.2,-0.2,-0.2,0)^i$	0.08				0.00*	1.00
16: $\tau^{-1}(-0.2,-1.2,0.8,0.8,-0.2,0)^i$	0.06	0.10			0.00*	1.00*
17: $\tau^{-1}(0.8,-0.2,0.8,-0.2,-1.2,0)^i$	0.02	0.21			0.00*	1.00*
18: $\tau^{-1}(0.2,-0.8,1.2,0.2,-0.8,0)^i$	0.10	0.21			0.00*	1.00*
19: $\tau^{-1}(0.4,-0.6,0.4,0.4,-0.6,0)^i$	0.16				0.42	0.58
20: $\tau^{-1}(0.4,0.4,0.4,-0.6,-0.6,0)^i$	0.04				0.11	0.89
21: $\tau^{-1}(0.2,-0.8,0.2,0.2,0.2,0)^i$	0.02				0.84	0.16
22: $\tau^{-1}(0.4,-1.6,0.4,0.4,0.4,0)^i$	0.55				0.16	0.84
23: $\tau^{-1}(1.8543,0,0,0,0,0)^i$	−0.12				0.00*	1.00*
24: $\tau^{-1}(0.4584,-0.6876,0.4521,0.3124,-0.5416,0)^i$	−0.21	−0.14			0.00*	1.00*
25: $\tau^{-1}(0.3124,-0.5416,0.4584,0.3124,-0.5416,0)^i$	−0.24	0.24			0.00*	1.00*
26: $\tau^{-1}(0,-1.2362,0,0,0,0)^i$	−0.57				0.00*	1.00*
OD3: $\mathbf{x}_0=(-0.2,-0.2,-0.2,-0.2,-0.25)$			0.90	0.10		
27: $(0,0,0,0,0,0)^i$					1.00	0.00
28: $\tau^{-1}(-0.4,-0.4,0.6,0.6,-0.4,0)^i$	0.01				1.00	0.00
29: $\tau^{-1}(0.2,0.2,0.2,0.2,-0.8,0)^i$	0.03				1.00	0.00
30: $\tau^{-1}(0.6,-0.4,-0.4,0.6,-0.4,0)^i$	0.02				1.00	0.00
31: $\tau^{-1}(0.4,-0.6,0.4,0.4,-0.6,0)^i$	0.14				0.76	0.24
32: $\tau^{-1}(1.2,-0.8,-0.8,0.2,0.2,0)^i$	−0.13	−0.02			1.00	0.00
33: $\tau^{-1}(-0.8,-0.8,1.2,1.2,-0.8,0)^i$	0.12				1.00	0.00
34: $\tau^{-1}(0.2,0.2,1.2,0.2,-1.8,0)^i$	0.00	0.48			1.00	0.00
35: $\tau^{-1}(0,-1,0,1,0,0)^i$	0.05	−0.01			1.00	0.00
36: $\tau^{-1}(1,0,0,0,-1,0)^i$	0.26	0.05			0.00	1.00
37: $\tau^{-1}(0,1,1,1,-1,0)^i$	−0.37				0.00	1.00
38: $\tau^{-5}(0.6,-0.4,-0.4,0.6,-0.4,0)^i$	−0.08				1.00	0.00

TABLE III. (*Continued.*)

Subdomain: $\mathbf{x}^i$	u_1 (Å)	u_2 (Å)	$B_\parallel$ (Å^2)	$B_\perp$ (Å^2)	p(TM)	p(Al)
OD4: $\mathbf{x}_0=(-0.4,-0.4,-0.4,-0.4,-0.25)$			2.10	2.04		
39: $(0,0,0,0,0,0)^i$					0.47	0.53
40: $\tau^{-1}(-0.2,0.8,0.8,-0.2,-1.2,0)^i$	−0.04				0.00*	1.00*
41: $\tau^{-1}(0.2,0.2,0.2,0.2,-0.8,0)^i$	0.02				0.00*	1.00*
42: $\tau^{-1}(1.2,-0.8,-0.8,0.2,0.2,0)^i$	−0.01				0.00*	1.00*
43: $\tau^{-1}(0.2,-0.8,0.2,1.2,-0.8,0)^i$	−0.25	−0.11			0.00*	1.00*
44: $\tau^{-1}(0.8,-1.2,-0.2,0.8,-0.2,0)^i$	0.70	0.09			0.00*	1.00*
45: $\tau^{-1}(0.6,-0.4,-0.4,0.6,-0.4,0)^i$	−0.09				0.10	0.90
46: $\tau^{-1}(-0.4,-0.4,0.6,0.6,-0.4,0)^i$	−0.94				0.00*	1.00*
47: $\tau^{-1}(0.8,-0.2,-0.2,-0.2,-0.2,0)^i$	−0.08				0.28	0.72
48: $\tau^{-1}(1.6,-0.4,-0.4,-0.4,-0.4,0)^i$	0.34				0.00*	1.00*
49: $\tau^{-1}(0,0,0,0,-1.8543,0)^i$	0.65				0.00*	1.00*
50: $\tau^{-1}(0,0.4584,0,-0.5055,0.8763,0)^i$	−0.69	0.03			0.00*	1.00*
51: $\tau^{-1}(1.2362,0,0,0,0,0)^i$	0.26				0.00*	1.00*
OD5: $\mathbf{x}_0=(0,0,0,0,-0.25)$			0.40	0.40		
52: $(0,0,0,0,0,0)^i$					0.21	0.79
53: $\tau^{-1}(0.6,-0.4,-0.4,-0.4,0.6,0)^i$	0.10				0.30	0.70

$[|F_o|>3\sigma(|F_o|)]$, 177 unique reflections; $wR=0.201$ and $R=0.241$ for data set 2 with weak reflections $[|F_o|>1\sigma(|F_o|)]$, 780 unique reflections; and $wR=0.057$ and $R=0.081$ for data set 3 with strongest reflections $[|F_o|>10\sigma(|F_o|)]$, 85 unique reflections.

The maxima and minima of the residual electron density according to the difference Fourier maps in external space are $\Delta\rho^e_{max}=1.15$ eÅ^{-3} and $\Delta\rho^e_{min}=-0.88$ eÅ^{-3}, respectively. The corresponding values for the maxima and the minima of the full electron density are $\rho^e_{max}=43.54$ eÅ^{-3} and $\rho^e_{min}=-6.12$ eÅ^{-3}, respectively. Electron density maps calculated by the maximum-entropy method fully agree with the structure derived from the 5D model.

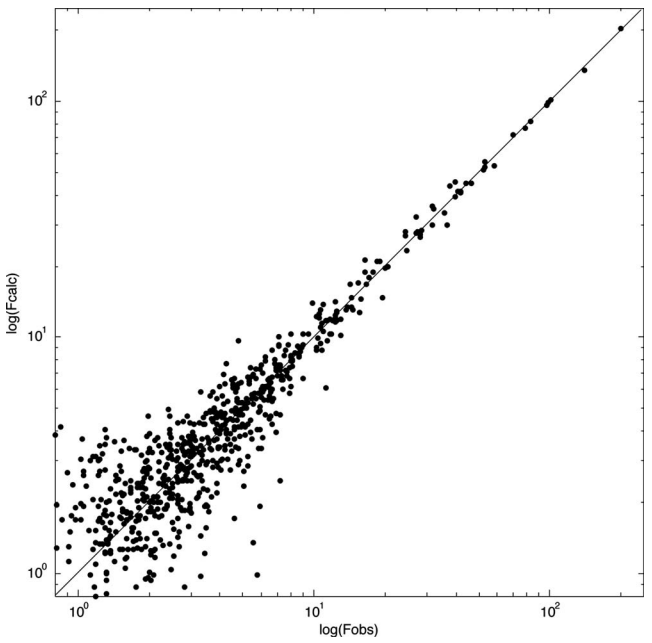

FIG. 3. F_{obs}/F_{calc} plot on a logarithmic scale for the final model of $Al_{72.5}Co_{18.5}Ni_9$ (957 reflections, $wR=0.123$, and $R=0.156$).

V. 3D STRUCTURE MODEL AND THE W PHASE

A 3D quasiperiodic structure model can be obtained as a particular irrational cut of the 5D hypercrystal structure with 3D external space. In Fig. 4, characteristic sections and a projection of the 3D structure are shown. The underlying tiling with an edge length of ≈4.8 Å marks the typical columnar clusters with ≈20 Å diameter (see also Fig. 5). One has to keep in mind that the choice of a fundamental cluster is not unique.[4,5] In the following, we will use the same kind of cluster that has been frequently employed for the description of the W phase[25] and the different modifications in d-Al-Co-Ni. However, the structure could be equally well described by the alternative generic cluster model.[26]

In our structure model, only one type of cluster can be identified that is oriented always in the same way as it is the case for the W phase,[27] which is a rational approximant. The cluster centers decorate the vertices of a pentagon tiling with ≈20 Å edge length [Fig. 4(c)]. The main difference between the current structure and the model of the d-Al-Co-Ni superstructure of type I (S1) (Ref. 28) is that in the latter the clusters occur in two orientations and do not feature a central atom.

The structures of basic Co-rich d-Al-Co-Ni and the W phase are built from the same fundamental ≈20 Å cluster. It

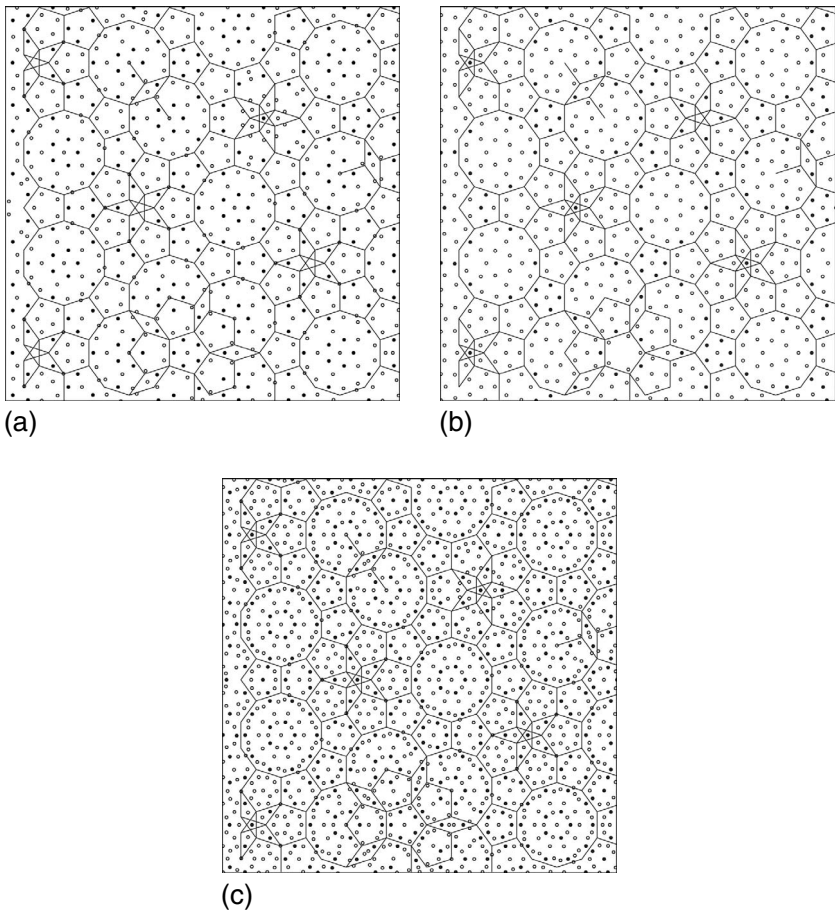

FIG. 4. Atomic layers at (a) $x_3=3/4$, (b) $x_3=1/4$, and (c) projection along the tenfold axis of the average structure of decagonal $Al_{72.5}Co_{18.5}Ni_9$ (70×70 Å^2). White and black circles correspond to Al and TM atoms, respectively. In case of mixed atomic sites, the majority component is indicated.

consists of a decagon surrounded by ten pentagons. In the layer at $x_3=3/4$, an Al atom is surrounded by five TM atoms followed by a large Al pentagon and subsequently by a 15-gon of five TM and ten Al atoms. The layer at $x_3=1/4$ is rotated by $\pi/5$ relatively to the former and the innermost atomic shell consists of an Al pentagon without a central atom.

These two layers are similar to the layers (A plus A′) and B in the W phase (see Fig. 6). The Al atoms at layer x_3

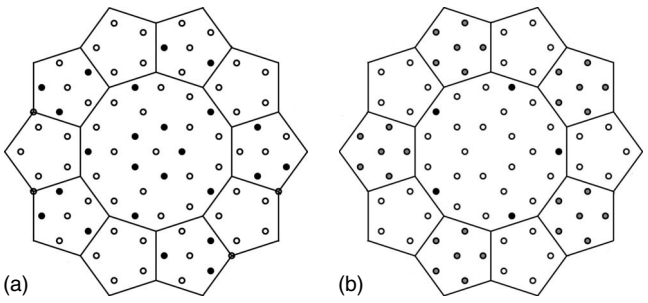

FIG. 5. Atomic layers at (a) $x_3=3/4$ and (b) $x_3=1/4$ of the ≈20 Å cluster of the average structure with two-layer periodicity. Open and filled circles correspond to Al and TM atoms, respectively, and gray-shaded circles indicate mixed occupied positions. The shortest interatomic distances are ≈2.5 Å

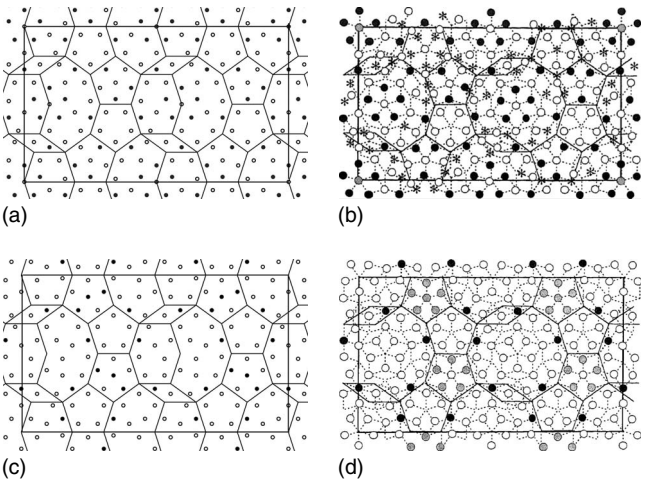

FIG. 6. Layers of the W phase as derived from basic Co-rich d-$Al_{72.5}Co_{18.5}Ni_9$ [(a) and (c)] compared to [(b) and (d)] its actual structure (Ref. 25); $x_3=3/4$ for [(a) and (b)] and $x_3=1/4$ for [(c) and (d)]. The layer in (b) is combined from layers A and A′, related by *C* centering, of the W phase. The differences between layers at A and at A′ are indicated by asterisks. Wherever atoms are to close to each other in this combined layer, these are partially occupied split positions. White and black circles correspond to Al and TM atoms, respectively, and gray circles indicate mixed occupied positions.

=3/4, related to the averaged layers A and A′ in the W phase, exhibit larger displacements from their ideal positions. The maximal shifts we observed for the Al subdomains 44, 46, and 50, reach each ≈1 Å, while those occupied by TM are maximum 0.16 Å.

Since the W phase[25] [space group *Cm*, a=39.668(3) Å, b=8.158(1) Å, c=23.392(1) Å, and β=90.05(1)°] is a rational approximant, its structure can be directly obtained from the 5D structure of basic Co-rich d-$Al_{72.5}Co_{18.5}Ni_9$ by applying a particular linear phason strain. For this purpose, we have to use the basis of the four-layer superstructure embedding since the W phase has a four-layer structure as well. We have also to take into account that a rational approximant of the two-layer average structure of the d phase can only give the two-layer average structure of the W phase, which has space group *Pm* and only half the lattice parameter in a direction.

The 5D unit cell of the superstructure is five times larger than that of the average structure[28] (ten times if we consider the doubling of the period along the tenfold axis). Therefore, we first have to transform the basis of the average structure into that of the superstructure. The reciprocal basis vectors of the superstructure, $\mathbf{d}_j^*$ (j=1,…,5), are related to those of the average structure, $\mathbf{d}_{0j}^*$ by $\mathbf{d}_j^*=\Sigma_j T_{ij}\mathbf{d}_{0j}^*$ with

$$T=\frac{1}{5}\begin{pmatrix} 2 & -1 & 1 & -2 & 0 \\ 2 & 4 & 1 & 3 & 0 \\ -3 & -1 & 1 & -2 & 0 \\ 2 & -1 & 1 & 3 & 0 \\ 0 & 0 & 0 & 0 & 5/2 \end{pmatrix}.$$

The resulting quasilattice parameters are a_o'=5.221 Å and c_o'=8.144 Å (along the tenfold axis). The lattice vectors of the approximant can be determined[29] to $\mathbf{a}_{app}=\tau^k\mathbf{a}_o'$, $\mathbf{c}_{app}=\tau^{k'}a_o'(\mathbf{a}_1-\mathbf{a}_4)$, and $\mathbf{b}_{app}=\mathbf{c}_o'$ along tenfold axis of the quasicrystal. Then $a_{app}=|\mathbf{a}_{app}|=\tau^k|\mathbf{a}_o^p|$, $c_{app}=|\mathbf{c}_{app}|=2\cos(\pi/10)\tau^{k'}|\mathbf{a}_o^p|$, where $|\mathbf{a}_o^p|=\frac{2}{\sqrt{5}}|\mathbf{a}_o'|$=4.670 Å. Then, we obtain for the lattice parameters of the two-layer average structure of the W phase k=3 and k'=2 so that $a_{app}=\tau^3|\mathbf{a}_o^p|$=19.782 Å and $c_{app}=2\cos(\pi/10)\tau^2|\mathbf{a}_o^p|$=23.256 Å.

In other terms, it can be written as

$$\mathbf{a}_{app}=p\mathbf{a}_0+q(\mathbf{a}_1+\mathbf{a}_4), \tag{5}$$

$$\mathbf{c}_{app}=r(\mathbf{a}_1-\mathbf{a}_4)+s(\mathbf{a}_2-\mathbf{a}_3). \tag{6}$$

Substituting in Eq. (5) the lattice constants of the approximant and of the quasicrystal we obtain p=3 and q=2. And for Eq. (6) the parameters result to r=2 and s=1. Hence we have a rational $\langle 3/2,2/1\rangle$ approximant, defined by the ratio of two consecutive Fibonacci numbers. The Fibonacci series is generated by the recursion relation: $F_{k+1}=F_k+F_{k-1}$ where F_0=0 and F_1=1. In our case $p=F_{k+1}$, $q=F_k$, $r=F_{k'+1}$, and $s=F_{k'}$.

Based on these results the required phason strain matrix can be calculated to $\mathbf{H}=\mathbf{I}+\mathbf{H}'$ where $\mathbf{I}$ is the unit matrix and $\mathbf{H}'$ contains coefficients in the bottom-left 2×2 block. For the current case of $\langle F_{k+1}/F_k, F_{k'+1}/F_{k'}\rangle$, the nonvanishing matrix coefficients are $\delta_1=-(-1/\tau^2)^k=0.0557[=\tau(q\tau-p)/(q+p\tau)]$ and $\delta_2=(-1/\tau)(-1/\tau^2)^{k'}=-0.0902[=(s\tau-r)/(s+r\tau)]$.

Taking into consideration the space group of the W phase, we determined the origin of the section with the five-dimensional space to be $(10\bar{1}\bar{1}0)^i/2$. The resulting structure of the approximant is shown in Fig. 6. Similar to the average structure of the decagonal $Al_{72.5}Co_{18.5}Ni_9$, the average structure of the W-phase approximant has only two different layers along the b axis. Consequently the layer at z=3/4 is an average of layers A and A′ in the real W-phase structure and, consequently, it contains a number of split positions. The translation period along the axes a_{app} and b_{app} of the created approximant are half of the original values in the W phase. Therefore we have an average structure of the W phase with the a_{app}^{av}=19.884 Å, b_{app}^{av}=4.069 Å, and c_{app}^{av}=23.375 Å. It is rotated by $\pi/10$ to that of the average structure of the quasicrystal presented in Fig. 4 since they are defined by different bases.

VI. CONCLUSIONS

In this first step of the structure solution of basic Co-rich d-$Al_{72.5}Co_{18.5}Ni_9$, its two-layer average structure could be successfully determined. As could be anticipated from the respective electron micrographs and x-ray diffraction patterns, it is closely related to the d-Al-Co-Ni superstructure of type I (S1) and to the structure of d-Al-Fe-Ni. This allowed to use a modified structure model, originally proposed for d-Al-Fe-Ni,[17] as starting model for the refinements.

An important result of this study is that the average structure of the W phase can be directly obtained as rational approximant of the average structure of basic Co-rich d-$Al_{72.5}Co_{18.5}Ni_9$. This has the consequence that we can use the structure of the W phase in the 5D embedding to design a starting model for the determination of the full four-layer structure. This first-structure solution of the full four-layer structure will enhance our understanding of the complex ordering phenomena in the system Al-Co-Ni.

ACKNOWLEDGMENTS

We thank Cesar Pay Gomez and Thomas Weber for helpful discussions and gratefully acknowledge financial support by the Swiss National Science Foundation under Grant No. SNF 200020-105158. We also acknowledge support by the staff of the Swiss-Norwegian beamline (SNBL) at ESRF.

*angelica.strutz@mat.ethz.ch
†yamamoto.akiji@nims.go.jp
‡walter.steurer@mat.ethz.ch

[1] W. Steurer and D. Sutter-Widmer, J. Phys. D **40**, R229 (2007).
[2] W. Steurer and S. Deloudi, Acta Crystallogr. A **64**, 1 (2008).
[3] W. Steurer, J. Non-Cryst. Solids **334–335**, 137 (2004).
[4] W. Steurer, Philos. Mag. **86**, 1105 (2006).
[5] C. L. Henley, M. de Boissieu, and W. Steurer, Philos. Mag. **86**, 1131 (2006).
[6] W. Steurer, Z. Kristallogr. **219**, 391 (2004).
[7] S. Ritsch, C. Beeli, H. U. Nissen, T. Gödecke, M. Scheffer, and R. Lück, Philos. Mag. Lett. **78**, 67 (1998).
[8] S. Katrych and W. Steurer, Z. Kristallogr. **219**, 606 (2004).
[9] K. H. Hassdenteufel, A. R. Oganov, S. Katrych, and W. Steurer, Phys. Rev. B **75**, 144115 (2007) and references cited therein.
[10] K. Hiraga, Adv. Imaging Electron Phys. **122**, 2 (2002).
[11] H. Takakura, A. Yamamoto, and A. P. Tsai, Acta Crystallogr. A **57**, 576 (2001).
[12] A. Cervellino, T. Haibach, and W. Steurer, Acta Crystallogr. B **58**, 8 (2002).
[13] H. Takakura, A. Yamamoto, and A. P. Tsai, Ferroelectrics **305**, 257 (2004).
[14] W. Steurer, T. Haibach, B. Zhang, S. Kek, and R. Lück, Acta Crystallogr. B **49**, 661 (1993).
[15] A. Yamamoto, K. Kato, T. Shibuya, and S. Takeuchi, Phys. Rev. Lett. **65**, 1603 (1990).
[16] A. Strutz and W. Steurer, Philos. Mag. **87**, 2747 (2007).
[17] A. Yamamoto and S. Weber, Phys. Rev. Lett. **79**, 861 (1997).
[18] A. Yamamoto, Acta Crystallogr. A **52**, 509 (1996).
[19] A. Yamamoto, Sci. Technol. Adv. Mater. **9**, 013001 (2008).
[20] K. Edagawa, M. Ichihara, K. Suzuki, and S. Takeuchi, Philos. Mag. Lett. **66**, 19 (1992).
[21] A. Yamamoto and K. N. Ishihara, Acta Crystallogr. A **44**, 707 (1988).
[22] H. Takakura, A. Yamamoto, M. Shiono, T. J. Sato, A. P. Tsai, J. Alloys Comp. **342**, 72 (2002).
[23] S. Deloudi, Ph.D. thesis No. 18107, ETH Zurich (2008).
[24] D. Schwarzenbach, Acta Crystallogr. A **45**, 63 (1989).
[25] K. Sugiyama, S. Nishimura, and K. Hiraga, J. Alloys Compd. **342**, 65 (2002).
[26] S. Deloudi and W. Steurer, Philos. Mag. **87**, 2727 (2007).
[27] K. Hiraga, T. Ohsuna, W. Sun, and K. Sugiyama, Mater. Trans. **42**, 2354 (2001).
[28] A. Yamamoto, H. Takakura, and E. Abe, Phys. Rev. B **72**, 144202 (2005).
[29] K. Niizeki, J. Phys. A **24**, 3641 (1991).